Combined Monte Carlo and Molecular Dynamics Simulation of Fully Hydrated Dioleyl and Palmitoyl-oleyl Phosphatidylcholine Lipid Bilayers

S. W. Chiu,* Eric Jakobsson,* Shankar Subramaniam,* and H. Larry Scott#

*Department of Molecular and Integrative Physiology, Department of Biochemistry, UIUC Programs in Biophysics, Neuroscience, and Bioengineering, and Beckman Institute, University of Illinois, Urbana, Illinois 61801; and #Department of Physics, Oklahoma State University, Stillwater, Oklahoma 74078 USA

ABSTRACT We have applied a new equilibration procedure for the atomic level simulation of a hydrated lipid bilayer to hydrated bilayers of dioleyl-phosphatidylcholine (DOPC) and palmitoyl-oleyl phosphatidylcholine (POPC). The procedure consists of alternating molecular dynamics trajectory calculations in a constant surface tension and temperature ensemble with configurational bias Monte Carlo moves to different regions of the configuration space of the bilayer in a constant volume and temperature ensemble. The procedure is applied to bilayers of 128 molecules of POPC with 4628 water molecules, and 128 molecules of DOPC with 4825 water molecules. Progress toward equilibration is almost three times as fast in central processing unit (CPU) time compared with a purely molecular dynamics (MD) simulation. Equilibration is complete, as judged by the lack of energy drift in 200-ps runs of continuous MD. After the equilibrium state was reached, as determined by agreement between the simulation volume per lipid molecule with experiment, continuous MD was run in an ensemble in which the lateral area was restrained to fluctuate about a mean value and a pressure of 1 atm applied normal to the bilayer surface. Three separate continuous MD runs, 200 ps in duration each, separated by 10,000 CBMC steps, were carried out for each system. Properties of the systems were calculated and averaged over the three separate runs. Results of the simulations are presented and compared with experimental data and with other recent simulations of POPC and DOPC. Analysis of the hydration environment in the headgroups supports a mechanism by which unsaturation contributes to reduced transition temperatures. In this view, the relatively horizontal orientation of the unsaturated bond increases the area per lipid, resulting in increased water penetration between the headgroups. As a result the headgroup-headgroup interactions are attenuated and shielded, and this contributes to the lowered transition temperature.

INTRODUCTION

Recent experimental studies of lipid bilayers (Nagle et al., 1996; Tristram-Nagle et al., 1998; Weiner and White, 1992a,b) have produced increasingly detailed pictures of the structure of fluid phase lipid bilayers at the level of mean positions and conformations of constituent molecular groups. Studies of dioleyl-phosphatidylcholine (DOPC) bilayers have examined the atomic level structure of these systems in states of partial hydration (Weiner and White, 1992a,b) and full hydration (Tristram-Nagle et al., 1998). These precise experiments yield structure details in bilayers that arise from the complex set of intermolecular interactions. The only theoretical approach capable of probing the nature of the interactions between atoms on lipid and water molecules, and the mechanisms by which these interactions lead to the observed structures, is computer simulation. By doing simulations that are consistent with available experimental data, we gain an atomic level structural and dynamical picture of the system. Predicted velocities and coordinates averaged over many simulation steps are used to calculate macroscopic properties of the model, which can be directly linked to the macroscopic behavior observed in experiments. Extension of the database of predictions from simulations to a wider class of biologically relevant lipid systems is the aim of the work presented here. This work also adds to the foundation on which simulations of more complex systems, including lipid-cholesterol and lipid-protein systems, can be designed.

Atomic level simulations of lipid bilayers of dipalmitoyl phosphatidylcholine (DPPC) and other lipid bilayers have been carried out by several groups over the past several years (Venable et al., 1993; Stouch, 1993; Eggberts et al., 1994; Damodaran and Merz, 1994; Feller et al., 1994, 1997; Heller et al., 1993; Huang et al., 1994; Armen et al., 1998; Chiu et al., 1995; Tu et al., 1995; Tieleman and Berendsen, 1996; Berger et al., 1997; Husslein et al., 1998). Several reviews of simulation methods and results have been published (Pastor, 1994; Roux and Merz, 1996; Tieleman et al., 1997; Jakobsson, 1997). While most of the simulations to date have been of DPPC bilayers, Heller et al. (1993) carried out a simulation of a POPC bilayer using stochastic boundary conditions and ~27 waters/lipid. Armen et al. (1998) recently carried out a simulation of a POPC bilayer with 13.5 waters per lipid using constant lateral area, temperature, and applied normal pressure (NPAT). In both of the simulations the number of waters is lower than that of full hydration (~32 waters/lipid) so that a simulation of POPC at full hydration has not heretofore been reported. Experimental structural data for fully hydrated POPC bilayers are currently limited to order parameter profiles (Seelig and Waespe-Šarčevič, 1978).

Received for publication 5 May 1999 and in final form 29 July 1999.

Address reprint requests to Dr. Hugh L. Scott, Jr., Dept. of Physics, Oklahoma State University, Stillwater, OK 74078-0444. Tel.: 405-744-5796; Fax: 405-744-6811; E-mail: physhis@okstate.edu.

0006-3495/99/11/2462/08 $2.00

TABLE 1 6–12 Parameters for interactions between atoms on different chains

	CH_2		CH_3	
	σ (nm)	ϵ (kJ/m)	σ (nm)	ϵ (kJ/m)
Saturated Carbons (CH_2, CH_3)	0.400	0.380	0.351	0.570
Unsaturated Carbons (CH)	0.375	0.380		

Previous simulations of DOPC were reported by Huang et al. (1994) and Feller et al. (1994). In the former, simulations were of a very small system (a total of 12 lipid molecules and ~22 waters per lipid per leaflet) at low hydration. The latter simulations were focused on the low hydration bilayers studied experimentally by Weiner and White (1992a, b). Now that detailed structural data for DOPC at a number of different levels of hydration are available (Tristram-Nagle et al., 1998; Hristova and White, 1998) it is appropriate to do a simulation of this system. In this work we have considered fully hydrated DOPC. Simulations of partially hydrated DOPC will be reported in a future paper.

A major problem in systems as complex as lipid bilayers is reaching equilibrium in finite computational time scales (Pastor and Feller, 1986). In less heterogeneous systems, such as proteins, it is possible to begin from crystal structure configurations, which are similar to configurations in the natural environment and rapidly evolve the system to equilibrium using molecular dynamics (MD) or Monte Carlo (MC) methods. In lipid membrane systems crystal structures are highly ordered, and therefore are far from equilibrium relative to the fluid-like physiological state. A new approach to equilibrating lipid membranes by expansion from a crystal phase has recently been developed by our group (Scott et al., 1998; Chiu et al., 1999). The procedure involves successive 20-ps MD runs at constant temperature and pressure (or surface tension), followed by 5000 steps of configurational bias Monte Carlo (CBMC) (Seipmann and Frenkel, 1992) on the lipids only, at constant volume and temperature. CBMC moves are followed by reinsertion of the water molecules, energy minimization to remove any bad lipid-water contacts caused during the CBMC and the next round of MD, and so on. We previously applied the method to a long simulation of a DPPC bilayer and have shown that the MD-CBMC simulation evolves much more quickly to the fluid phase. Each CBMC interval utilized ~1/3 of the CPU time as the intervening MD runs, and we found an overall speed-up by a factor of ~2.6 in CPU time over purely MD for the expansion and equilibration of the fluid lipid. Equilibration was verified by noting that the potential energy of the system stabilized quickly after CBMC runs and remained very stable during three independent 200-ps intervals of continuous MD, for a total of 600 ps (Chiu et al., 1999).

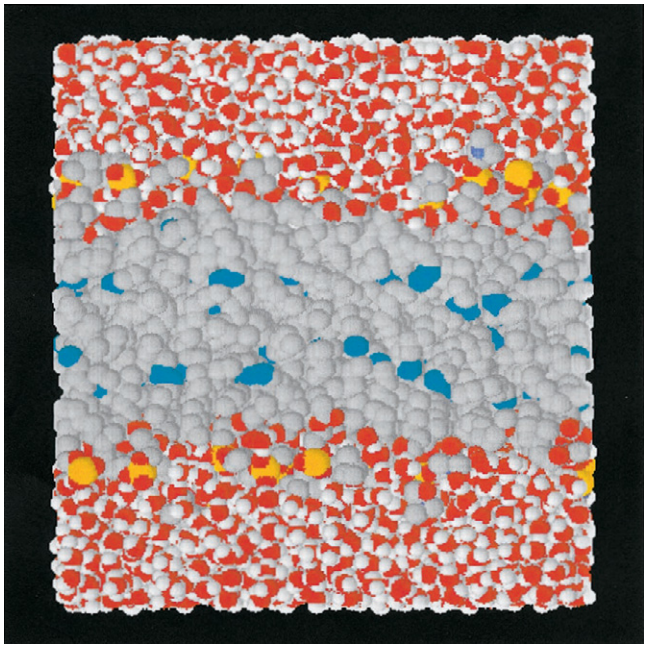

FIGURE 1 Snapshot of a fully equilibrated hydrated POPC bilayer. Water molecules are color-coded red (H) and white (O). Lipid methyls and methylenes are color-coded gray. C═C atoms are color-coded cyan. Headgroup P atoms are yellow, and headgroup N atoms are blue.

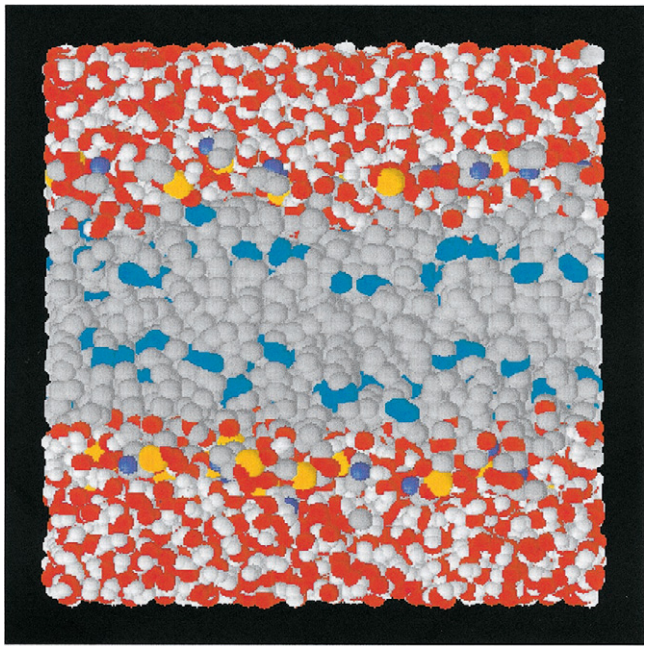

FIGURE 2 Snapshot of a fully hydrated equilibrated DOPC bilayer. Color-coding is the same as in Fig. 1.

The purpose of this paper is to describe the results of application of the MD-CBMC method to fully hydrated POPC and DOPC bilayers. In the following sections we describe the details of the simulations, and present the results.

SIMULATION METHODS AND PROCEDURES

We constructed a bilayer patch consisting of 128 POPC molecules, 64 in each leaflet, and 4628 water molecules. The initial phase of the bilayer is

TABLE 2 Calculated and experimental structural data for POPC and DOPC

	POPC (expt)	POPC (calc)	DOPC (expt)	DOPC (calc)
Volume/mol (Å^3)	1267	1263 ± 10	1303	1288 ± 10
Headgroup separation (Å)		34 ± 2	35.3	34 ± 2
Area/mol (Å^2)		66.4 ± 1	72.2	71.0 ± 1

Experimental data from Nagle and Weiner, 1988; Tristram-Nagle et al., 1998.

an ordered structure, with coordinates of each lipid generated from energy-minimized POPC tetramer coordinates given to us by C-H. Huang (Li and Huang, 1996). Then cycles consisting of 30 ps of MD followed by 5000 CBMC steps were run on this system using a temperature of 425 K. The MD was run using the NγT algorithm, which we employed in earlier MD simulations of dimyristoyl phosphatidylcholine (DMPC) and DPPC (Chiu et al., 1995, 1999), using the GROMOS simulation code (BIOMOS b.v., Laboratory of Physical Chemistry, ETH Zentrum Universitatstrasse 6, CH-8092 Zurich, or see http://igc.ethz.ch/gromos/). The surface tension was 46 dynes/cm. The CBMC steps were run at the same temperature, and at a fixed volume equal to that at the end of the preceding MD step. For computational efficiency reasons, water molecules are not moved during CBMC. This necessitates reinsertion of the water after each CBMC run, and energy minimizing to remove any unphysical contacts that may have resulted from CBMC moves to the lipid headgroups. We have found (Chiu et al., 1999) that this latter step requires only a few minutes of computer time and generally only a few water molecules are repositioned. The subsequent MD cycle began with velocities assigned from a Boltzmann distribution at 425 K. We emphasize that MD and CBMC steps are carried out in different thermodynamic ensembles, rather like a textbook quasi-static expansion with a small expansion followed by a constant volume equilibration followed by another small expansion, and so on.

After the system expanded to an area per molecule of 69 Å^2 per lipid, the temperature was lowered to 325 K for further CBMC/MD cycles. When the system contracted to an area of 67 Å^2 per lipid we began a continuous MD run of 200 ps for the calculation of structural data. The continuous MD simulation was done in an NPAT ensemble, in which the area per molecule was constrained to fluctuate around 67 Å^2 per lipid, a pressure of 1 atm was applied normal to the bilayer, and the temperature was constrained to fluctuate around 325 K. All boundary constraints utilized the weak coupling method (see BIOMOS above) with a coupling constant of 0.2 ps for temperature, 4.0 ps for pressure scaling, and 2.0 ps for area scaling. Temperature coupling was applied separately to lipid and water components. After this simulation was finished a CBMC run of 5000 steps was done, followed by reinsertion of the water molecules and energy minimization. Then another 210-ps, NPAT, MD run was done. Discarding the first 10 ps to allow for equilibration after CBMC, this procedure was repeated again to give a total of three separate 200-ps trajectories which were then used for averaging. We found that equilibration after CBMC occurred very rapidly, and 10 ps was more than sufficient for this purpose as judged by the behavior of the potential energy versus time.

For the DOPC simulation we began with the POPC bilayer we obtained at the end of the expansion phase described above, with area equal to 69 Å^2 per lipid. Two additional carbon atoms were added to the 2-chain, and a double bond replaced the single bond at the 9 position in this chain for each lipid molecule. Due to anticipated further expansion, a few additional waters were added, making the total number of waters 4825. The system was subjected to 12 further cycles of MD/CBMC at 425 K. Then the temperature was lowered to 325 K for six additional MD/CBMC cycles. After this, three continuous NPAT MD runs of 200 ps, separated by CBMC as in the case of POPC, were done, giving a total of three independent 200-ps trajectories for averaging. The area for the NPAT MD runs was constrained to 70 Å^2 per lipid, with pressure equal to 1 atm and temperature equal to 325 K.

Interaction parameters for water and lipid headgroups, and intramolecular interactions, were the same as those we used earlier (Chiu et al., 1999), namely the GROMOS96 set. For computing torsion angle motions around saturated bonds, third-neighbor 6-12 interactions were replaced with the dihedral potential function according to Ryckaert and Bellmans (1975). For the hydrocarbon chain interactions between atoms on different chains, we utilized a new set of parameters developed by our group by fitting to densities of a series of alkanes and, for the C═C double bond, to 5-decene (Chiu et al., 1999b). The values for these parameters are given in Table 1. Spherical cutoffs of 20 Å for both electrostatics for 6-12 forces were used. In the CBMC runs electrostatic interactions were modulated by the continuum dielectric constant of water. We have discussed the rationale for these choices earlier (Chiu et al., 1999).

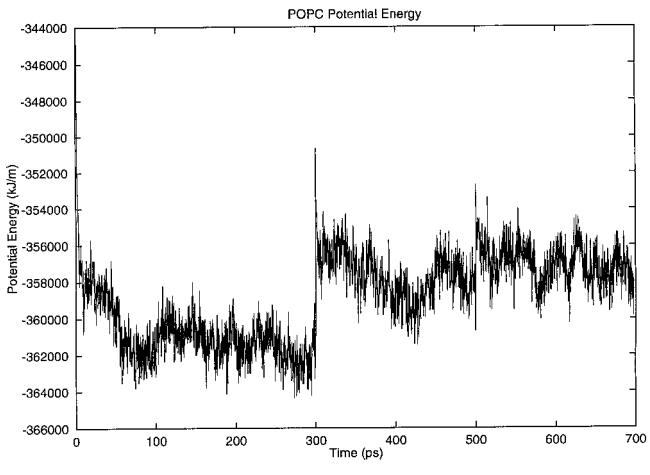

FIGURE 3 Plot of potential energy versus time for the POPC continuous MD trajectory that started from the end of the final CBMC/MD equilibration step. Discontinuities at 300 ps and at 500 ps occur after CBMC runs.

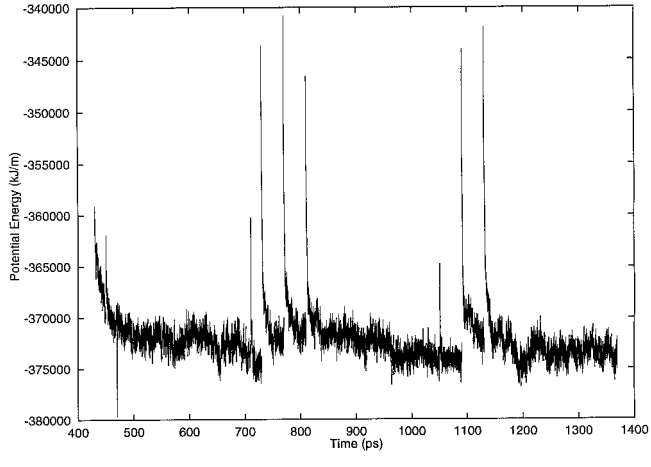

FIGURE 4 Plot of potential energy versus time for the DOPC continuous MD trajectory that started from the end of the final CBMC/MD equilibration step. Initial steps are not plotted, so the time axis is different from Fig. 3. Discontinuities occur after CBMC runs.

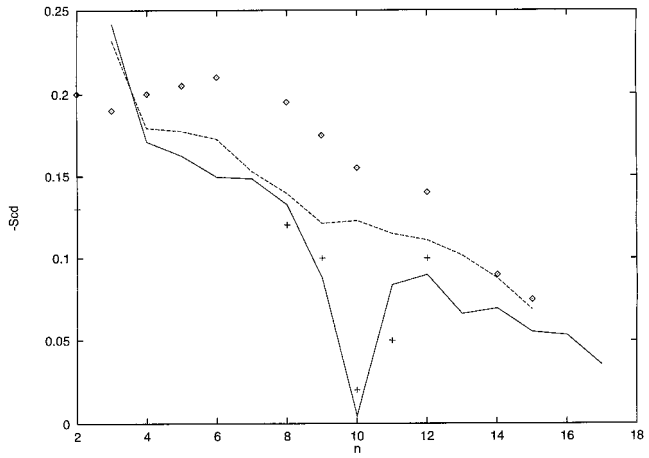

FIGURE 5 Plot of order parameters for POPC, calculated from averages over the 3 × 200 ps continuous MD runs. *Solid line:* calculated profile for the *sn*-1 chain. *Dashed line:* calculated profile for the *sn*-2 chain. *Diamonds and crosses:* experimental profiles for *sn*-1 and *sn*-2, respectively (Seelig and Waespe-Šarčevič, 1978).

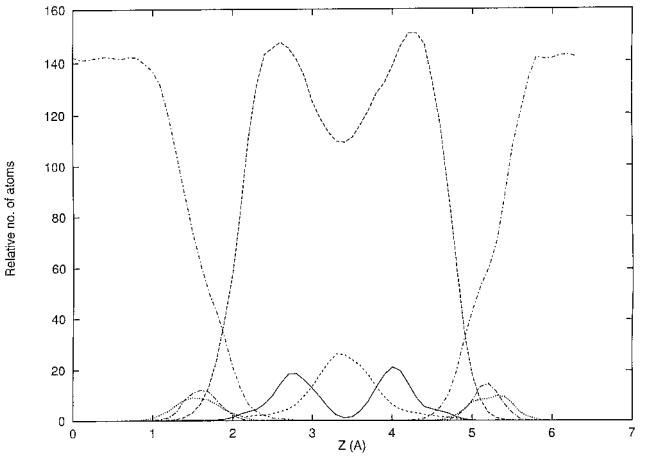

FIGURE 7 Atom distributions across the bilayer for POPC: *dot-dash,* water O; *large dash,* chain CH2; *small dash,* chain CH3; *solid line,* C═C; *dot,* P; *dot-dash,* N. Vertical scale is number of atoms per 1-Å slab, and horizontal scale denotes location of slab.

RESULTS

Figs. 1 and 2 show fully expanded, hydrated, fluid-phase POPC and DOPC bilayers which our simulation produced. The molecular volumes V_L of both POPC and DOPC were calculated from the simple relation (Petrache et al., 1997)

$$V_L = AD/2 - N_W V_W$$

where A is the area per molecule and D the width of the simulation box. N_W is the number of waters, and V_W is the volume per water, taken to be 30.4 Å^3 (Petrache et al., 1997). We find that $V_{POPC} = 1263$ Å^3, in excellent agreement with the value determined by Armen et al. (1998). For DOPC we find $V_{DOPC} = 1288$ Å^3, in excellent agreement with experimental data (Tristram-Nagle et al., 1998) and data from a simulation at lower hydration (Armen et al., 1998). Table 2 summarizes structural properties of the simulated bilayers.

Equilibration for these bilayers is demonstrated in Figs. 3 and 4, which are plots of potential energy versus time for POPC and DOPC, respectively. In Fig. 3, there is no systematic discernible drift in the potential energy data, but there is a discontinuity that occurred after a CBMC run at the 300 ps point. The effect of CBMC at this point has been to cause the system to undergo a jump in configuration space to another stable region. At the 500 ps point there is a smaller change in the potential energy of the system. The net change is ~2% of the total potential energy of the system, and did not produce noticeable changes in any average structural properties of the system that we were able to observe. The most likely origin of the change is the lipid-water interface, where a headgroup move may have

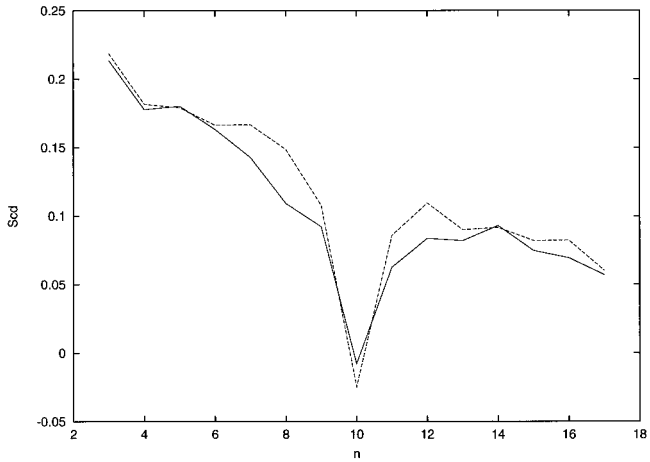

FIGURE 6 Plot of order parameters for DOPC, calculated from averages over the 3 × 200 ps continuous MD runs. *Solid line: sn*-1 chain, *dashed line: sn*-2 chain.

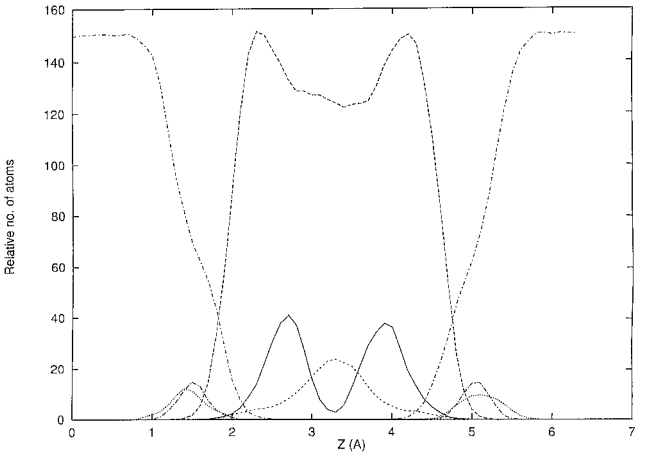

FIGURE 8 Atom distribution profiles across the bilayer for DOPC: *dot-dash,* water O; *large dash,* chain CH2; *small dash,* chain CH3; *solid line,* C═C; *dot,* P; *dot-dash,* N. Vertical scale is number of atoms per 1-Å slab, and horizontal scale denotes location of slab.

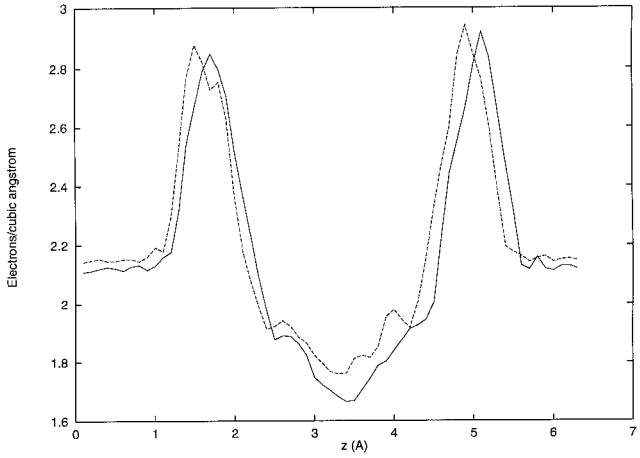

FIGURE 9 Plot of electron densities for POPC and DOPC, averaged over continuous MD runs. *Solid curve:* POPC; *dashed curve:* DOPC.

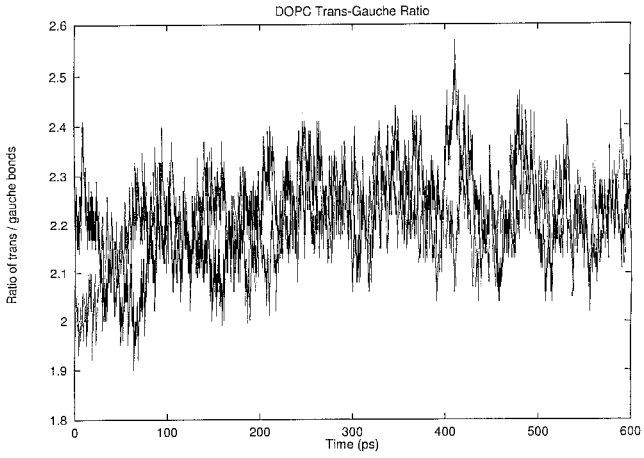

FIGURE 11 Plot of the ratio of *trans* bonds to *gauche* bonds for DOPC as a function of time over the continuous MD run. *Solid line: sn*-1 chain; *gray line: sn*-2 chain.

occurred during CBMC moves that then produced a localized redistribution of water molecules. Fig. 3 shows that in both cases the system remains stable in energy through the subsequent 200-ps continuous MD run. For POPC, the three segments used for averaging are at 100–300 ps, 300–500 ps, and 500–700 ps. Fig. 4 reveals a more complex situation for DOPC. The large spikes in the potential energy curve are due to unfavorable headgroup-water contacts after CBMC. This was more problematic for DOPC due to the larger area per molecule. Fig. 4 shows that, after only a few picoseconds of MD, the total potential energy for the system returns to near its original value, and there is no over-arching drift in Fig. 4. For DOPC, the three segments used for averaging are at 500–700 ps, 900–1100 ps, and 1200–1400 ps.

Fig. 5 shows the order parameter profile calculated for the POPC simulation. Also shown are the experimental data of Seelig and Waespe-Šarčevič (1978). While the agreement is very good for the unsaturated *sn*-1 chain, calculated order parameters for the saturated *sn*-2 chain are somewhat lower than those in the experiment. It seems natural that order should be less in the *sn*-2 chain than in, say, a DPPC bilayer, due to the disordering effect of the double bond as noted by the deep dip in S_n at $n = 10$. This effect is evident in our data where order parameters for both chains are nearly equal except at the double bond position.

Fig. 6 shows the order parameter profile calculated from the 200-ps segment of the uninterrupted MD trajectory for the DOPC simulation. While there are no experimental data for direct comparison for this system, we note the effect of the double bonds is the same for both chains. Overall, order parameters are lower for DOPC than for POPC, reflecting the larger area per molecule and smaller membrane thickness for this system.

Figs. 7 and 8 show calculated atom distributions for both POPC and DOPC bilayers, respectively. Comparison of the figures shows that the primary difference is in the methylene distribution. In DOPC, the dip in this data in the center

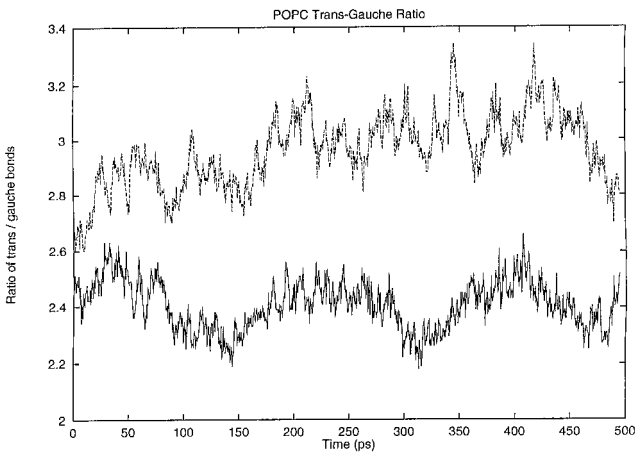

FIGURE 10 Plot of the ratio of *trans* bonds to *gauche* bonds for POPC as a function of time over the continuous MD run. *Solid line: sn*-1 chain; *dashed line: sn*-2 chain.

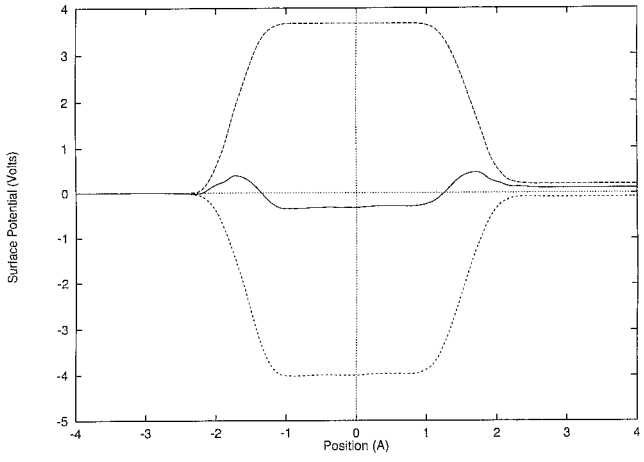

FIGURE 12 Plot of the dipole potential profile across the bilayer for POPC. *Top curve:* contribution from lipid headgroups. *Bottom curve:* contribution from water molecules. *Middle curve:* net potential difference.

of the bilayer is less pronounced than in POPC. Close examination of Figs. 7 and 8 also reveals somewhat deeper penetration of water molecules in the DOPC bilayer compared with POPC. The profiles are very similar, with the exceptions of broader C═C peaks for DOPC and very slightly more widely separated heads, as indicated by peaks in the headgroup nitrogens.

Fig. 9 compares electron density profiles for POPC and DOPC on the same plot. Electron densities were calculated by placing the appropriate number of electrons at the cites of the atomic nuclei, and then binning over the entire simulation cell. The peak-to-peak distance for both POPC and DOPC is 34 ± 2 Å, which is close to the value of 35.3 Å measured for hydrated DOPC by Tristram-Nagle et al. (1998). For the DOPC plot, the separation of the methyl shoulders (distance between the peaks of the shoulders) is ~12 Å, also in excellent agreement with the data of Tristram-Nagle et al. The figure emphasizes the overall similarity in structure of the POPC and DOPC systems.

Figs. 10 and 11 show plots of the ratio of *trans* to *gauche* bonds versus time for POPC and DOPC, respectively. The effect of unsaturation is clear in comparison of the pictures. The 2-chain of POPC has a consistently higher ratio of *trans* bonds to *gauche* bonds, reflecting the higher degree of order that is also evident in the calculated order parameter profile for that chain.

Figs. 12 and 13 show the surface dipole potential profile across the bilayers for POPC and DOPC, respectively. Both bilayers exhibit the characteristic positive potential barriers between the aqueous exterior and the hydrocarbon interior of the membranes. In both cases the barrier is the result of a small difference between the competing orientations of water dipoles (negative) and headgroup dipoles (positive). In the case of POPC the average height of the barrier is ~325 mV, while the average barrier height for DOPC is 180 mV. In both cases, the separate contributions of water and phospholipid were similar (4 V).

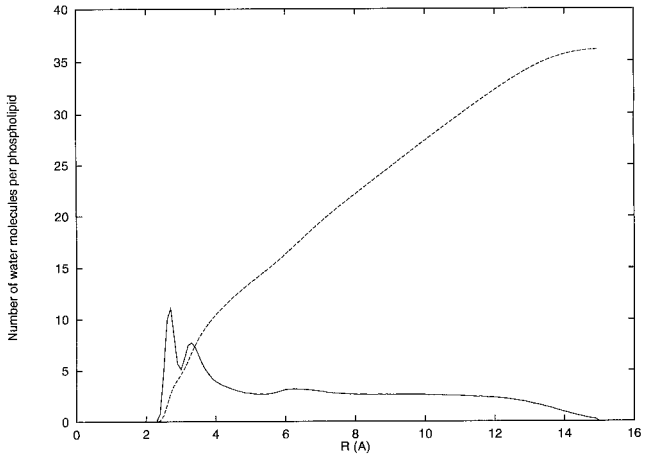

FIGURE 14 Plot of the radial distribution function (RDF) of the distance to the nearest lipid headgroup for the water molecules in the POPC simulations. *Solid line:* RDF; *dashed line:* integral of the RDF.

Figs. 14 and 15 show plots of the radial distribution function (RDF) of the distance to the nearest lipid headgroup for the water molecules in the simulations. The RDFs were calculated by simply finding the nearest lipid headgroup atom for each water molecule, and binning the resulting distribution of distances. Normalization was defined so that the integral of the RDF over the system gave the total number of waters, as the figures indicate. Also plotted are the integrals of the RDFs. The figures show a double peak, which indicates the presence of two layers of water molecules in the interfacial region. The first peak represents an average distance of ~2.5 Å from headgroups, indicative of tightly bound water. The second represents an average distance of ~3.6 Å. The peaks in DOPC and POPC RDFs are at the same radial locations, but the main peak is sharper and higher for DOPC compared with POPC. The secondary peak in the DOPC RDF is also slightly higher than the second peak in the POPC RDF. In earlier simulations of

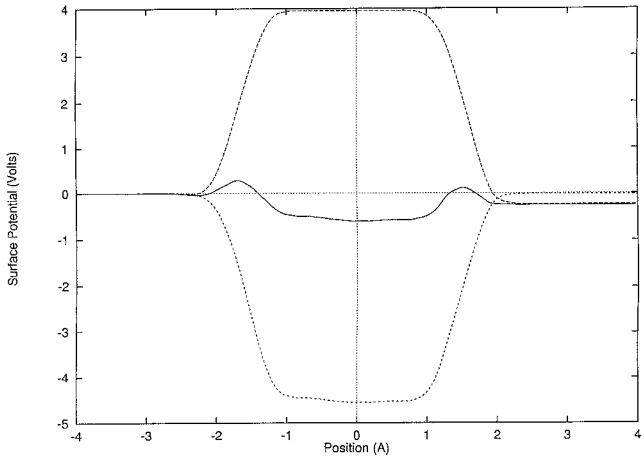

FIGURE 13 Plot of the dipole potential profile across the bilayer for DOPC. *Top curve:* contribution from lipid headgroups. *Bottom curve:* contribution from water molecules. *Middle curve:* net potential difference.

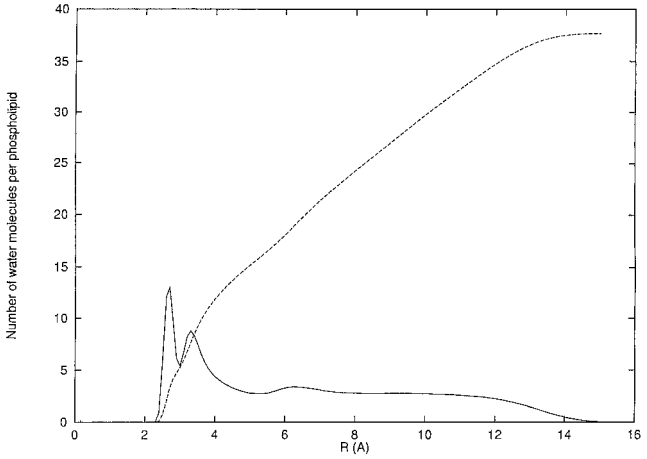

FIGURE 15 Plot of the radial distribution function (RDF) of the distance to the nearest lipid headgroup for the water molecules in the DOPC simulations. *Solid line:* RDF; *dashed line:* integral of the RDF.

DMPC (Chiu et al., 1995) we observed a single peak in the RDF at ~3 Å. The double peak occurs when the area per lipid is larger. In this case the lipid molecules begin to have two distinct hydration layers around them, instead of just one.

DISCUSSION

Table 2 compares calculated and experimental structural data from the simulations. By fixing the area to fluctuate around the chosen values of 67 $Å^2$ for POPC and 71 $Å^2$ for DOPC, the molecular volumes and headgroup spacings are in good agreement with experimental values. The other data available for comparison are the order parameters for POPC. From Fig. 5 it is evident that the order parameter profile agrees with experimental data for the unsaturated *sn*-1 chain, with the exception of the single experimental data point at $n = 2$. For the saturated *sn*-2 chain our calculations predict a more disordered chain than is seen experimentally in PC lipids with two saturated chains. Intuitively this seems reasonable, since increased disorder in the unsaturated chain, and consequently increased area per lipid, should induce some increase in disorder in the neighboring saturated chains, although the data of Seelig and Waespe-Šarčevič (1978) do not show this effect.

The simulations clearly show the effect of increased area per molecule in PC lipid bilayers. Bilayers with larger area per headgroup have a lower surface dipole potential (Figs. 12 and 13), and water molecules are able to penetrate the headgroup region in greater numbers so that a second layer of hydration appears (Figs. 14 and 15), compared to bilayers with lowered area per molecule. The number of waters that are in clearly defined hydration layers around lipid headgroups is greater for DOPC due to the greater area per molecule.

A striking result of the simulations is the overall similarity in many ways of the POPC and DOPC bilayers, despite the difference in the 2-chain structure. The electron density and atom distribution profiles are remarkably similar, suggesting that the increased disorder in DOPC produced by the extra C═C bond on the 2-chains is compensated by the addition of two extra methyls to that chain. The increased area per molecule for DOPC is sufficiently small that changes in separation of the headgroup positions normal to the membrane plane are barely noticeable in Figs. 7 and 8, and are undetectable in the electron density plots (Fig. 9). Given that DOPC has a lower phase transition temperature than POPC or DPPC, we speculate that the biological importance of unsaturated lipids such as DOPC is not to change bilayer dimensions, but rather to maintain fluidity over a larger temperature range *without* disrupting the bilayer thickness or overall distribution of atoms. Figs. 14 and 15 show that one means by which introduction of double bonds reduces the chain melting phase transition temperature is to increase the number of waters that contact the lipid headgroups, thereby shielding interactions between the heads. Interestingly, while the two saturated-chain lipids, dipalmitoyl phosphatidylcholine (DPPC) and dipalmitoyl phosphatidylethanolamine (DPPE), have phase transitions that differ by ~20°C, their di-unsaturated analogs, DOPC and DOPE, have phase transitions that are nearly identical (Berde et al., 1980).

These are the first simulations of fully hydrated POPC and DOPC bilayers. They extend the database of predictions from simulations to a wider class of biologically relevant lipid systems. The simulation data provide an atomic level picture of the effect of unsaturation on the structure of lipid bilayers. We have found for these simulations that our CBMC/MD simulation procedure produced well-equilibrated bilayers with predicted order parameters, electron densities, molecular volumes, and atom distributions that agree well with available experimental data for these systems. The simulations provide insight into the effects of double bonds on chain packing and on headgroup interactions with water.

We thank V. Balaji for his contributions in optimizing the CBMC code.

This work was supported by National Institutes of Health Grant GM54651 (to E.J. and H.L.S.) and National Science Foundation Grant MCB 96-31050 (to E.J.).

REFERENCES

Armen, R. S., O. D. Uitto, and S. E. Feller. 1998. Phospholipid component volumes: determination from bilayer structure calculations. *Biophys. J.* 75:734–744.

Berde, C. B., H. C. Andersen, and B. S. Hudson. 1980. A theory of the effects of head group structure and chain unsaturation on the chain melting transition of phospholipid dispersions. *Biochemistry.* 19: 4279–4293.

Berger, O., O. Edholm, and F. Jahnig. 1997. Molecular dynamics simulations of a fluid bilayer of dipalmitoylphosphatidylcholine at full hydration, constant pressure, and constant temperature. *Biophys. J.* 72: 2002–2013.

Chiu, S.-W., M. Clark, E. Jakobsson, S. Subramaniam, and H. L. Scott. 1999. Application of a combined Monte Carlo and molecular dynamics method to the simulation of a dipalmitoyl phosphatidylcholine lipid bilayer. *J. Comp. Chem.* 20:1153–1164.

Chiu, S.-W., M. Clark, E. Jakobsson, S. Subramaniam, and H. L. Scott. 1999b. Optimization of hydrocarbon chain interaction parameters: application to the simulation of fluid phase lipid bilayers. *J. Phys. Chem.* B103: 6323–6327.

Chiu, S.-W., M. Clark, S. Subramaniam, H. L. Scott, and E. Jakobsson. 1995. Incorporation of surface tension into molecular dynamics simulation of an interface: a fluid phase lipid bilayer membrane. *Biophys. J.* 69:1230–1245.

Damodaran, K. V., and K. M. Merz. 1994. A comparison of DMPC and DLPE-based lipid bilayers. *Langmuir.* 9:1179–1183.

Eggberts, E., S. J. Marrink, and H. J. C. Berendsen. 1994. Molecular dynamics simulation of a phospholipid membrane. *Eur. Biophys. J.* 222: 423–436.

Feller, S. E., D. Yin, R. W. Pastor, and A. D. MacKerrell, Jr. 1997. Molecular dynamics simulation of unsaturated lipid bilayers at low hydration: parameterization and comparison with diffraction studies. *Biophys. J.* 73:2269–2279.

Feller, S. E., Y. Zhang, and R. W. Pastor. 1994. Computer simulation of liquid/liquid interfaces II. Surface tension-area dependence of a bilayer and monolayer. *J. Chem. Phys.* 103:10267–10276.

Heller, H., M. Schaefer, and K. Schulten. 1993. Molecular dynamics simulation of a bilayer of 200 lipids in the gel and in the liquid-crystal phase. *J. Phys. Chem.* 97:8343–8360.

Hristova, K., and S. H. White. 1998. Determination of the hydrocarbon core structure of fluid dioleylphosphocholine bilayers by x-ray diffraction using specific bromination of the double bonds: effect of hydration. *Biophys. J.* 74:2419–2433.

Huang, P., J. J. Perez, and G. H. Loew. 1994. Molecular dynamics simulations of phospholipid bilayers. *J. Biomol. Struct. Dyn.* 11:927–956.

Husslein, T., D. M. Newns, P. C. Pattnaik, Q. Zhong, P. B. Moore, and M. Klein. 1998. Constant pressure and temperature molecular dynamics simulation of the hydrated diphytanolphosphatidylcholine lipid bilayer. *J. Chem. Phys.* 109:2826–2832.

Jakobsson, E. 1997. Computer simulation studies of biological membranes: progress, promise, and pitfalls. *Trends Biochem. Sci.* 9:339–354.

Li, S., and C-H. Huang. 1996. Molecular mechanics simulation studies of dienoic hydrocarbons: from alkenes to 1-palmitoyl-2-linoleylphosphatidylcholines. *J. Comp. Chem.* 17:1013–1024.

Nagle, J. F., and M. C. Weiner. 1988. Structure of fully hydrated bilayer dispersions. *Biochim. Biophys. Acta.* 942:1–10.

Nagle, J. F., R. Zhang, S. Tristram-Nagle, W. Sun, H. Petrache, and R. M. Suter. 1996. X-ray structure determination of L_α phase DPPC bilayers. *Biophys. J.* 70:1419–1431.

Pastor, R. 1994. Molecular dynamics and Monte Carlo simulations of lipid bilayers. *Curr. Opin. Struct. Biol.* 4:443–464.

Pastor, R. W., and S. E. Feller. 1996. Time scales of lipid dynamics and molecular dynamics. *In* Biological Membranes: A Molecular Perspective from Computation and Experiment. K. M. Merz and B. Roux, eds. Birkhauser, Boston. 1–29.

Petrache, H. I., S. E. Feller, and J. F. Nagle. 1997. Determination of component volumes of lipid bilayers from simulations. *Biophys. J.* 72: 2237–2242.

Merz, K., and B. Roux, eds, 1996. Biological Membranes: A Molecular Perspective from Computation and Experiment. Birkhauser, Boston.

Ryckaert, J. P., and A. Bellmans. 1975. Molecular dynamics of liquid n-butane near its boiling point. *Chem. Phys. Lett.* 1975:123.

Scott, H. L., E. Jakobsson, and S. Subramaniam. 1998. Simulation of lipid membranes with atomic resolution. *Comput. Phys.* 12:328–334.

Seelig, J., and Waespe-Šarčevič. 1978. Molecular order in *cis* and *trans* unsaturated phospholipid bilayers. *Biochemistry.* 17:3310–3315.

Seipmann, I., and D. Frenkel. 1992. Configurational bias Monte Carlo: a new sampling scheme for flexible chains. *Mol. Phys.* 75:59–70.

Stouch, T. 1993. Lipid membrane structure and dynamics studied by all-atom molecular dynamics simulations of hydrated phospholipid bilayers. *Mol. Simul.* 10:317–335.

Tieleman, D. P., and H. J. C. Berendsen. 1996. Molecular dynamics simulations of a fully hydrated dipalmitoylphosphatidylcholine bilayer with different macroscopic boundary conditions and parameters. *J. Chem. Phys.* 105:4871–4880.

Tieleman, D. P., S. J. Marrink, and H. J. C. Berendsen. 1997. A computer perspective of membranes: molecular dynamics of lipid bilayer systems. *Biochim. Biophys. Acta.* 1331:235–270.

Tristram-Nagle, S., H. Petrache, and J. F. Nagle. 1998. Structure and interactions of fully hydrated dioleylphosphatidylcholine bilayers. *Biophys. J.* 75:917–925.

Tu, K., D. Tobias, and M. Klein. 1995. Constant pressure and temperature molecular dynamics simulation of a fully hydrated liquid crystal phase dipalmitoylphosphatidylcholine. *Biophys. J.* 69:2558–2562.

Venable, R., B. Zhang, B. Hardy, and R. Pastor. 1993. Molecular dynamics simulations of a lipid bilayer and of hexadecane: an investigation of membrane fluidity. *Science.* 262:223–226.

Weiner, M. C., and S. H. White. 1992a. Structure of a fluid dioleylphosphatidylcholine bilayer determined by joint refinement of x-ray and neutron diffraction Data II. Distribution and packing of terminal methyl groups. *Biophys. J.* 61:428–433.

Weiner, M. C., and S. H. White. 1992b. Structure of a fluid dioleylphosphatidylcholine bilayer determined by joint refinement of x-ray and neutron diffraction Data III. Complete structure. *Biophys. J.* 61: 433–447.